J Mol Model (2013) 19:3087–3094
DOI 10.1007/s00894-013-1839-3

ORIGINAL PAPER

Insight into the binding model of new antagonists of kappa receptor using docking and molecular dynamics simulation

Shiyuan Hu · Haijing Yu · Yongjuan Liu · Tian Xue · Huabei Zhang

Received: 15 January 2013 / Accepted: 25 March 2013 / Published online: 20 April 2013

Abstract PF-4455242 and its analogues represent a new series of kappa opioid selective antagonists that demonstrate high selectivity and potency. We investigated their binding mode to the κ-receptor via docking and molecular dynamics simulations. The ranking of the predicted binding free energies is consistent with experimental results. Detailed binding free energies between antagonists and individual protein residues were calculated, and key residues involved in binding were identified. Deviation of the active site residues was investigated, and the results show that Gln115, Leu135, Tyr139, Trp287 and Tyr313 deviate greatly from the reference structure. Information obtained from molecular modeling studies will aid in the design of potent kappa receptor antagonists.

Keywords Kappa receptor · Docking · Molecular dynamics simulation · MM-GB/SA

Introduction

The four opioid receptors, μ, δ, κ, and the nociceptin/orphanin FQ peptide receptor, belong to the class A (rhodopsin-like) γ subfamily of G-protein-coupled receptors (GPCRs), which are characterized by the presence of seven transmembrane helices, and are coupled predominantly to heterotrimeric G_i/G_o proteins in the intracellular domain [1, 2]. The μ, δ and κ opioid receptors are distributed widely in the central nervous system and, with opioids as ligands, are involved in a wide range of physiological symptoms such as pain perception, mood regulation, physical dependence and development of analgesic tolerance [3, 4]. Each opioid receptor type has selective agonists and antagonists that bind to and produce effects unique to that individual receptor type [5].

The kappa opioid receptor used to be considered as a promising target for pain, potentially lacking addiction/abuse liability. But most clinical trials were ended because of side effects [6]. Dysphoria, and strong diuresis are the most severe side effects associated with the application of kappa agonists. Dynorphin is the native peptide agonist at the kappa receptor, and changes in dynorphin levels in the nucleus accumbens in response to stress may be noteworthy. Most depressed patients exhibit a reduced ability to experience pleasure (anhedonia) and loss of motivation. Reward is mediated by the ventral tegmental area (VTA) nucleus accumbens (nAcc) dopaminergic pathway, which is modulated (inhibited) by the κ receptors located directly on dopaminergic containing cells that project to the nAcc. Dynorphin up-regulation in the nucleus accumbens shell is stimulated by stress and various drugs of abuse and causes anhedonia-like effects, potentially linking kappa antagonism as a path to treating depression. As a result, selective antagonists are of considerable interest as potential pharmacotherapies for addiction (cocaine, opiate, alcohol, nicotine, and possibly others), depression, anxiety disorders, obesity, and psychosis disorders [7]. Opioid antagonists with varying degrees of receptor potency and selectivity have been developed for the κ opioid receptor. PF-4455242 (Fig. 1, compound 11) and its analogues are a new series of kappa opioid selective antagonists reported by Verhoest and coworkers [16]. Compared to other antagonists, this series of compounds has two advantages: low molecular weight and moderate lipophilicity. Both properties are essential for ideal

Electronic supplementary material The online version of this article (doi:10.1007/s00894-013-1839-3) contains supplementary material, which is available to authorized users.

S. Hu · H. Yu · Y. Liu · T. Xue · H. Zhang (✉)
Key Laboratory of Radiopharmaceuticals of Ministry of Education, College of Chemistry, Beijing Normal University, Beijing 100875, China
e-mail: hbzhang@bnu.edu.cn

central nervous system drugs. PF-4455242 has entered phase 1 clinical testing. However, the binding model of these compounds to the κ-receptor still remains unclear. In this work, we selected six antagonists with different potency (Fig. 1) to explore the binding mode via docking and molecular dynamics (MD) simulations. The MM-GB/SA method was used to calculate the binding free energy, which helps us better understand the interaction between these small molecular antagonists and the protein. Detailed binding free energies between antagonists and individual protein residues were calculated using the MM-GBSA decomposition process.

Theory and methods

Antagonist structure

Sybyl-X 1.3 (http://www.tripos.com) was used to construct the original structure of these antagonists. The benzylic nitrogen atoms were modeled as ammonium states, so each entire molecule was positive charged. Geometry optimizations were performed using the Tripos force field with Gasteiger-Hückel charges and the Powell conjugate gradient algorithm. Thereafter, the structure was energy-minimized using Gaussian software [8] at the B3LYP/6-31G* level, and RESP charges were assigned to these inhibitors by the antechamber module in Ambertools12 package. The resulting structures were used for docking and dynamics studies.

Docking studies

A newly resolved X-ray structure of the kappa receptor and its antagonist JDTic was retrieved from the Protein Data Bank (PDB id:4DJH) [1]. There are two chains in the complex; chain A was used in this work. AutoDock 4.2 [9] was used to locate the appropriate binding orientations and conformations of the compounds into the binding pocket. The numbers of grid points in x,y,z were set to 70,70, 70 with the spacing value equivalent to 0.375 Å, and the center of the JDTic was regarded as the grid center. During docking, the number of docking runs was 150. The population in the genetic algorithm was 50, the number of energy evaluations was 250,000, and the maximum number of iterations was 27,000. Other parameters were set at the default values implemented by the program.

Molecular dynamics simulation

The κ-receptor crystal structure was determined using a κ-OR-T4 lysozyme (T4L) fusion protein (Fig. 2a), in which human κ-OR was engineered by fusing lysozyme from T4 phage (T4L) into ICL3 (Gly 261–Arg 263); the T4L was omitted in our simulations (Fig. 2b). The missing heavy atoms and missing residues Thr302–Thr306 and Val262 were modeled using Modeller 9v7 software [10]. Hydrogen atoms in the kappa receptor were added with the tleap module in the Amber software. Titratable residues other than Asp105 were left in their dominant protonation state at pH 7.0. Asp105, which is buried in the protein interior, was neutral in all simulations. Furthermore, the amino terminus Ser55 and the carbonyl terminus Pro347 were capped by an acetyl group (ACE) and an N-methyl group (NME), respectively. The prepared protein structures were inserted into an equilibrated palmitoyl-oleoyl-phosphatidylcholine(POPC) bilayer using vmd software [11]. All lipid molecules and waters with non-hydrogen atoms within 2 Å of the protein were deleted. The resulting membrane pdb file was processed by charmmlipid2amber.x provided by Ambertools12 and then combined with the protein. An appropriate amount of NaCL (0.15 nM) was added to the aqueous phase using tleap software. An appropriate number of chloride ions were added to the complex to neutralize the charges. The ff99SB and lipid11 force field were applied to produce force field parameters for the protein and the lipids, respectively.

All simulations were carried out using NAMD software. The particle mesh Ewald (PME) method [12] was applied to treat long-range electrostatic interactions with a periodic boundary condition, and bond lengths involving hydrogen atoms were constrained using SHAKE algorithm . The time-step for three MD simulations is 1 fs, with a direct-space, non-bonded cutoff of 10.0 Å . We performed energy minimization using the conjugate gradient method and a MD simulation for 200 ps with the solute positions restrained. We then performed 25 ns equilibration at 310 K with the protein restrained to relax the membrane. After that, different ligands were added to the system based on the docking results, waters with non-hydrogen atoms within 2 Å of the ligand were deleted, and one more chloride ion was added. The force field parameters of the small molecular antagonists, including the Lennard-Jones, torsion and bond angle terms, were assigned using the antechamber. The resulting systems had 258 lipid molecules, 57 sodium ions, 64 chloride ions, and about 20,000 water molecules, for a total of 100,000 atoms, and measured 105×105×110 $Å^3$ (Fig. 2c). After heating and equilibrium, a 10-ns isothermal isobaric ensemble (NPT)-MD simulation was applied to each system without any restraints. The temperature was regulated at 310 K using Langevin thermostat and the pressure was kept at 1.0 atm using isotropic positional scaling. The atom coordinates were collected at intervals of 1 ps for the last 10 ns to analyze the structures in detail. Finally, the root-mean-square deviation (RMSD) of protein backbone atoms

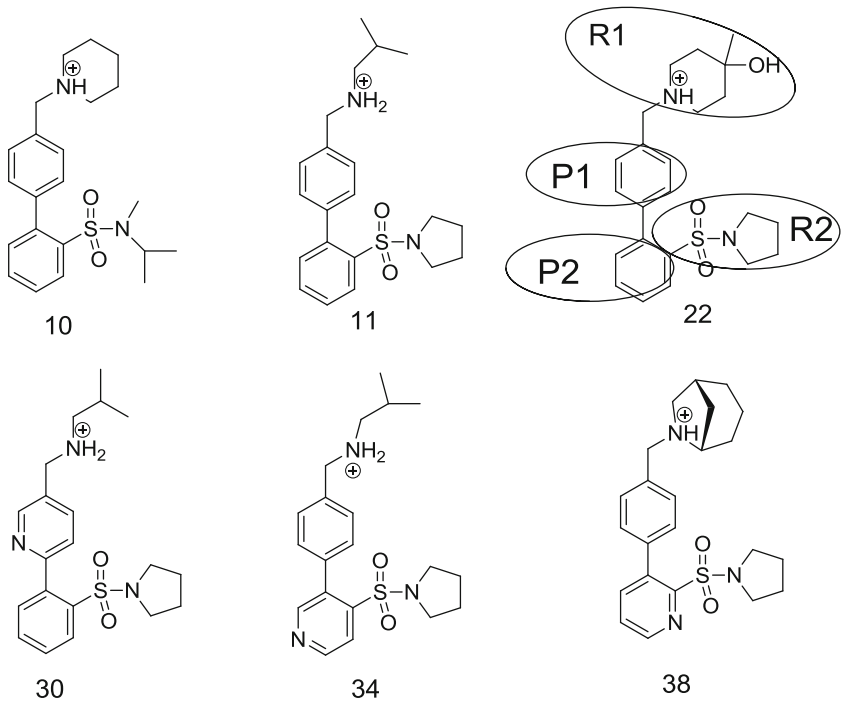

Fig. 1 Molecular structures of six opioid kappa (κ)-receptor antagonists

and antagonists was computed along the MD trajectory relative to the initial structures to determine the stability of the system.

MM-GBSA calculations

For each system, 100 snapshots were extracted from the last 2 ns along the MD trajectory at intervals of 20 ps for free energy calculations. The binding free energy of the antagonist to the κ receptor was calculated using the MM-GBSA method [13] in this work. In this method, the binding free energy ($\Delta G_{binding}$) can be represented as:

$$\Delta G_{binding} = G_{complex} - \left(G_{protein} + G_{lignd}\right) \quad (1)$$

The binding free energy ($\Delta G_{binding}$) is evaluated as the sum of the changes in the molecular mechanical (MM) gas-phase binding energy (ΔG_{MM}). The solvation free energy (ΔG_{solv}), and entropic ($-T\Delta S$) contribution

$$\Delta G_{binding} = \Delta G_{MM} + \Delta G_{solv} - T\Delta S \quad (2)$$

ΔG_{MM} is further divided into two parts: van der Waals (ΔE_{vdw}) and electrostatic energies (ΔE_{ele}). The solvation free energy (ΔG_{solv}) is further divided into a polar (ΔG_{pol}) and a nonpolar component (ΔGnonpol).

$$\Delta G_{MM=}\Delta E_{vdw} + \Delta E_{ele} \quad (3)$$

$$\Delta G_{solv} = \Delta G_{pol} + \Delta G_{nonpol} \quad (4)$$

ΔG_{pol} was computed using the pbsa program in Amber. The dielectric constant inside the solute was set to 1.0 and

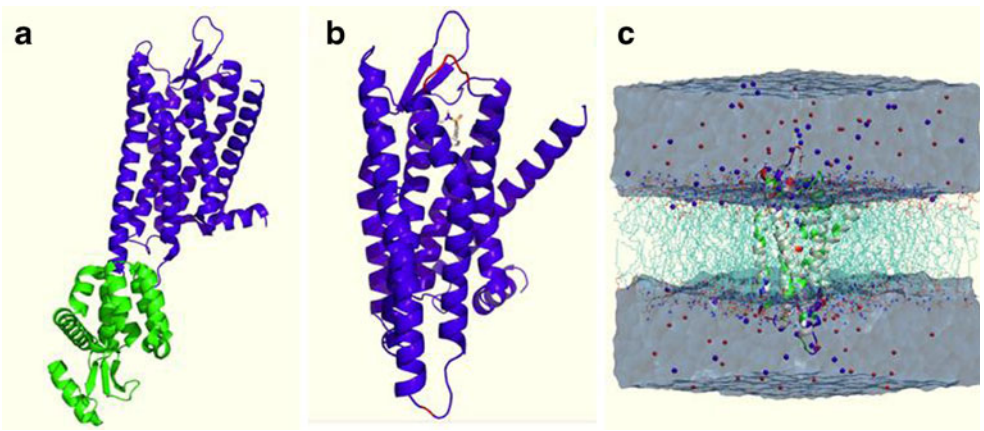

Fig. 2 **a** Structure of the kappa (κ) receptor and its antagonist (PDB id:4DJH) [1]. Chain A of 4DJH, T4L is in *green*. **b** Missing residues in the structural model for the κ receptor were completed with homology method (*red*). **c** The starting structural model for molecular dynamics (MD) simulation

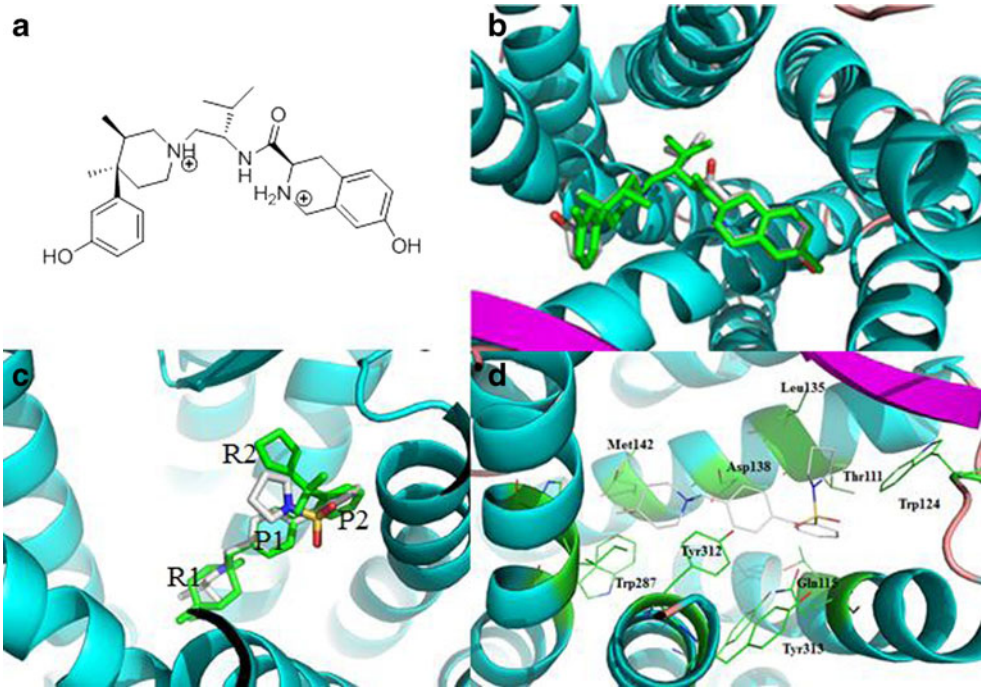

Fig. 3 **a** Structure of JDTic. **b** Conformational comparison of JDTic from the crystal structure (*green*) and that from the autodock 4.2 result (by atom type color). **c** Conformational comparison of compound 22 (*green*) and 11 (by atom type color). **d** Three-dimensional (3D) structural model of the main interactions between compound 22 and the κ receptor binding pocket

80.0 in the solvent in our calculations. ΔG_{nonpol} was calculated by:

$$\Delta G_{nonpol} = \gamma SASA + \beta \quad (5)$$

where SASA is the solvent-accessible surface area as determined by the MSMS program [14] with a probe radius of 1.4 Å. The values γ and β are empirical constants. We used 0.0072 kcal/(molÅ^2) and 0 kcal mol^{-1}, respectively. We chose a total number of 100 snapshots evenly from the last 2 ns on the MD trajectory with an interval of 20 ps.

Calculation of the inhibitor–residue interaction

The inhibitor–residue interaction, which is valuable to qualitatively define the binding mechanisms of the six antagonists to the kappa receptor, was analyzed using the MM-GBSA decomposition process. The binding interaction of each inhibitor–residue pair can be represented as:

$$\Delta G_{inhibitor-residue} = \Delta E_{vdw} + \Delta E_{ele} + \Delta G_{pol} + \Delta G_{nonpol} \quad (6)$$

In this equation, ΔE_{vdw} and ΔE_{ele} are non-bonded van der Waals interactions and electrostatic interactions, respectively. ΔG_{pol} and ΔG_{nonpol} are the polar and non-polar contributions to the inhibitor-residue interaction, respectively. The polar solvation contribution (ΔG_{pol}) is calculated using the pbsa program, and the parameters for the GB calculation were developed by Onufriev et al. [15]. All energy components were calculated using the same snapshots as the free energy calculation.

Results and discussion

Docking result

To determine the probable binding conformations of these antagonists, AutoDock4.2 was used to dock all compounds into the active sites of the κ receptor. The docking protocol was validated by re-docking. JDTic was removed from the active site and docked back into the binding pocket. The nitrogen atoms in both the piperidine and isoquinoline moieties of JDTic were treated as protonation states (Fig. 3a). The RMSD between the predicted conformation and the observed X-ray crystallographic conformation of JDTic was 0.52 Å (Fig. 3b). The small RMSD value indicated that the parameter set for the AutoDock simulation was reasonable to reproduce the X-ray structure. Therefore, the AutoDock method and the parameter set could be extended to search the binding conformations of other antagonists.

The docking approach was able to dock all of the antagonists into the active site with a similar pose (Fig. S4 in supporting information) with the exception of compound 11. The docked conformation of 11 is a little different from the others in that there is a dihedral angel between the two benzene rings (Fig. 3c). This will be discussed in detail in the next section. To elucidate the interaction mechanism, compound 22—one of the most potent antagonists—was selected for more detailed analysis. The best possible interacting model of compound 22 with the κ receptor and the main residues involved in the interaction are depicted generally in Fig. 3d. Compound 22 was docked into the

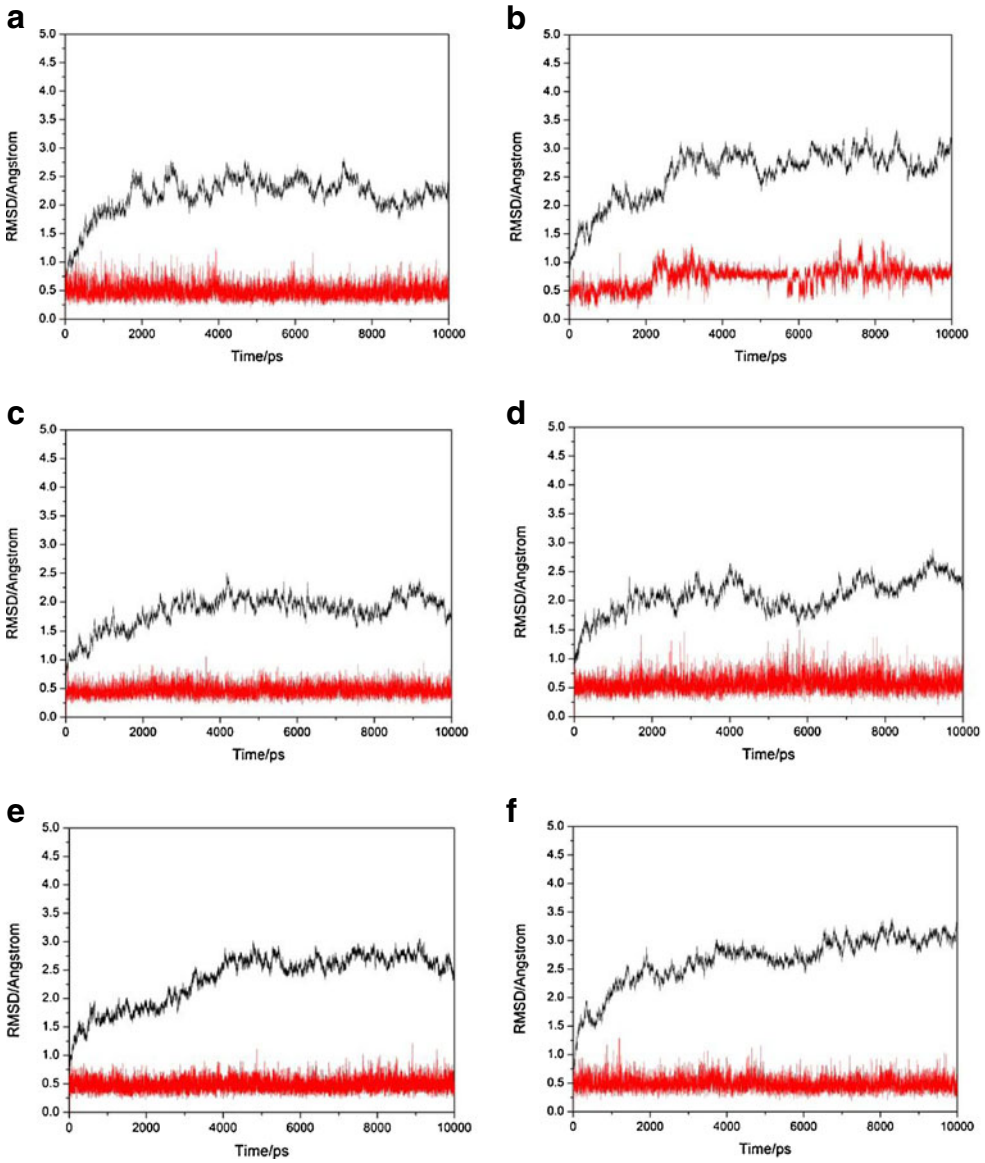

Fig. 4a–f Root-mean-square deviations (RMSD) of the κ receptor backbone atoms (*black*) and the ligand (*red*) relative to their initial minimized complex structures as a function of time. Ligands: **a** 10, **b** 11, **c** 22, **d** 30, **e** 34, **f** 38

binding site in such a way that its benzylic nitrogen atom forms an ionic interaction with the Asp138 side chain. The R1 group is placed in a hydrophobic sub-pocket formed by the side chains of Tyr139, Met142, Trp287, Ile290, His291 and Ile316. The biphenyl group interacts with the side chain of Leu135, Tyr312, Ile316, Tyr320 through hydrophobic interactions. Thr111, Gln115, Trp124 and Val134 form another sub-pocket; the R2 group locates to this pocket.

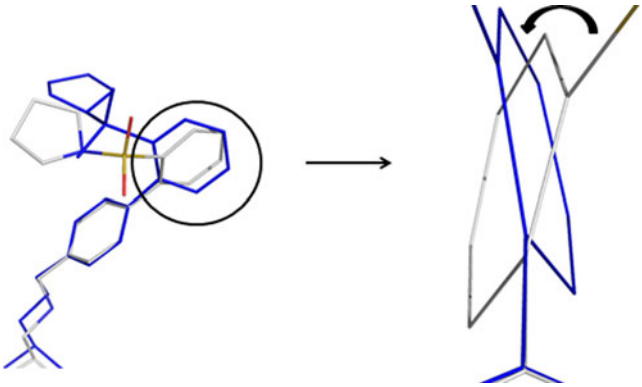

Fig. 5 Superimposed initial and final conformations of antagonist 11. The initial conformation is shown with different colors for different elements, the final conformation is shown in *blue*. *Right* Enlargement of the P2 group

Dynamic stability from MD

In this work, lipid bilayer simulations were carried out successfully for each system. The final 10-ns trajectory fragment was used for analyses. To evaluate the quality of our MD simulation, the RMSD values of the protein backbone atoms relative to the initial minimized structure during the phase of the simulation were calculated (plotted in Fig. 4). We can see that the six systems reached equilibrium after 3 ns of the simulation phase. This result shows that the

Table 1 Binding free energies computed by the MM-GBSA method[a]

Antagonist	ΔE_{vdw}	ΔE_{ele}	ΔG_{pol}	ΔG_{nonpol}	$\Delta G_{binding}$	ΔG_{expd}
10	−43.28±2.41	−86.96±8.16	100.75±7.46	−5.70±0.27	−35.18±2.49	−11.34
11	−46.04±2.94	−89.16±6.98	104.22±5.99	−6.73±0.15	−37.73±3.05	−12.08
22	−49.97±2.86	−66.90±6.95	84.19±6.25	−6.22±0.17	−38.92±2.70	−13.19
30	−40.56±2.95	−97.51±7.91	110.05±7.16	−6.29±0.24	−33.91±3.16	−9.65
34	−38.43±2.76	−90.60±6.94	106.95±5.91	−6.17±0.18	−28.25±3.26	−8.84
38	−43.12±2.87	−79.88±5.04	94.60±4.42	−6.20±0.14	−34.61±2.89	−10.32

[a] All values are given in kcal mol^{-1}

[b] $\Delta G_{binding} = \Delta Evdw + \Delta Eele + \Delta Gpol + \Delta Gnonpol$

[c] The experimental values ΔG_{exp} were derived from the experimental K_i values in Ref [16] using the equation $\Delta G \approx -RT \ln K_i$

trajectories of the MD simulations for the six complexes after equilibrium were reliable for post analyses.

One of the six antagonists (Fig. 4b, compound 11) exhibits increased RMSD after 2 ns, suggesting a conformational change during MD simulation. From the MD trajectory, we found that this conformation change was brought about by rotation of the P2 group. Figure 5 shows the superimposed initial and final conformations of antagonist 11. The dihedral angel between the two benzene rings changed from 75° to about 105°.

MM/GBSA calculation

To gain more insight into the inhibition mechanisms of the six small molecules at the atomic level, the MM-GBSA method was used to calculate binding free energies (Table 1). A total of 100 snapshots were taken at a time interval of 20 ps from the last 2 ns of the MD simulation for analyses of binding free energies.

The components of binding and solvation energies computed by MM-GBSA listed in Table 1 reveal that the binding free energies of compounds 10, 11, 22, 30, 34 and 38 to the κ receptor were −35.18, −37.73, −38.92, −33.91, −28.25 and −34.61 kcal mol^{-1}, respectively. The results are very good relative estimates of the antagonist binding affinities, with the correlation coefficient being 0.69 (Fig. 6). It is encouraging that the ranking of the experimental binding free energies is consistent with our predictions, which means that the current binding model is reliable.

According to the energy components of the binding free energies listed in Table 1, the major favorable contributors to inhibitor binding were van der Waals energies (ΔE_{vdw}). Non-polar solvation energies (ΔG_{nonpol}), which correspond to the burial of SASA upon binding, also made important contributions to binding. Although the electrostatic terms (ΔE_{ele}) favored antagonist binding, these favorable contributions were completely screened by the unfavorable stronger polar solvation energies (ΔG_{pol}). Furthermore, it should be noted that ΔE_{vdw} is much stronger than ΔG_{nonpol}. Therefore, van der Waals energies contribute most to binding of the antagonists with the κ receptor. Pyridyl analogues(30, 34, 38) showed ideal physicochemical properties and in

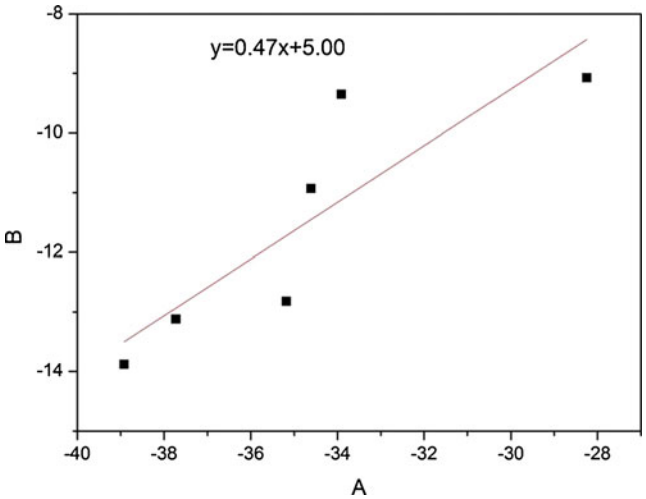

Fig. 6 Predicted- versus experimentally determined binding free energies of the six inhibitors. The correlation constant (R^2)= 0.69

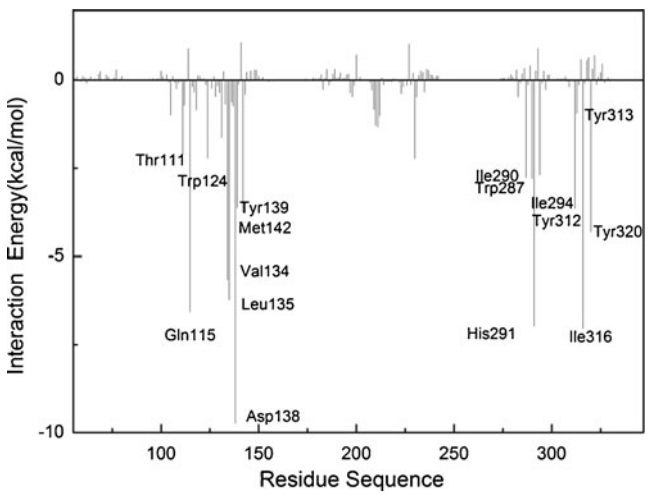

Fig. 7 Decomposition of $\Delta G_{binding}$ on a per-residue basis for C22-κ-receptor complexes

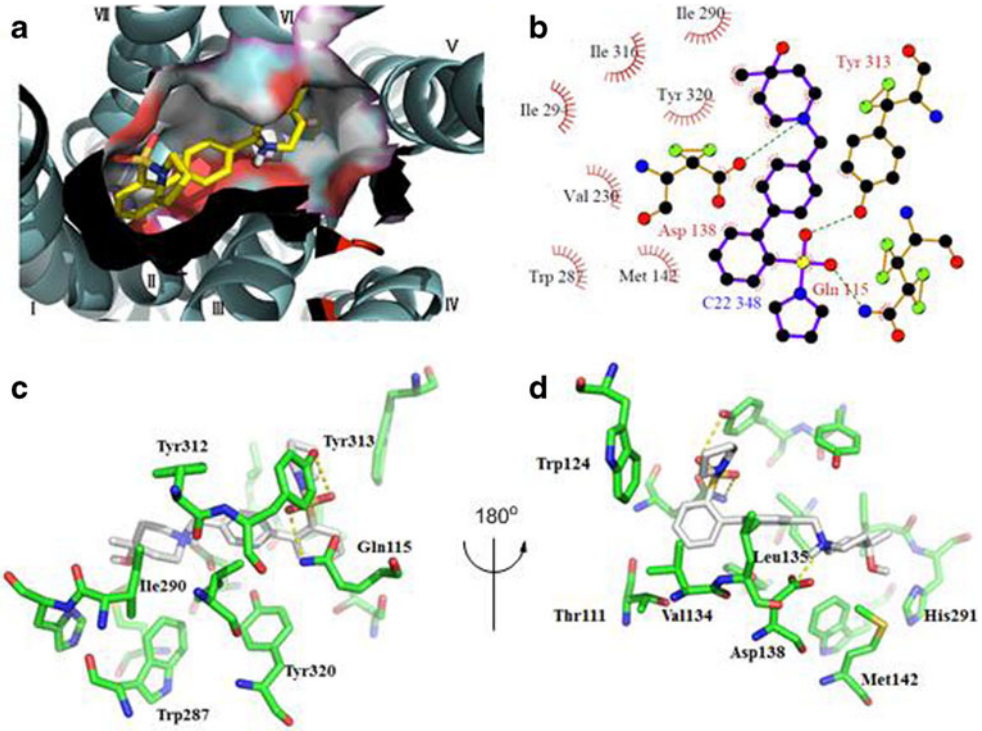

Fig. 8 **a**–**d** Geometries of key residues that produce favorable interactions with the six inhibitors are modeled in the complexes according to the lowest-energy structure from the MD trajectory for 22

vitro ADME, but low potency [16]. From Table 1, we found that the loss in potency is caused mainly by the low ΔE_{vdw} and stronger polar solvation energies. This result suggests that optimization of van der Waals interactions between antagonists and the κ receptor may lead to potent small molecule antagonists of the receptor.

Structure–affinity relationship

In order to better investigate the binding effect of the six antagonists, we analysed inhibitor–residue interaction energy decomposition using the MM-GBSA decomposition method. The antagonist–residue interaction spectrum for compound 22 was generated from the result of the analysis and was visualized in Fig. 7 (spectra for other systems is given in supporting information Fig. S1). The decomposition approach is useful not only to elucidate the binding mode at the atomic level, but also to locate residues that contribute to the receptor–antagonist interaction. At the same time, analysis of the structure and binding mode were carried out. Figure 8 plots the relative geometries of the compound 22 in the binding complex with the relevant residues on the basis of the lowest-energy structure from the MD trajectory. The structure shows a tight fit of the ligand in the bottom of the binding cleft, forming ionic, hydrogen-bond and extensive hydrophobic interactions with the receptor.

Table 2 RMSD values of active site residues

Residue	RMSD	Residue	RMSD
Thr111	1.45	Trp287	2.38
Gln115	1.90	Ile290	0.56
Trp124	1.21	His291	1.12
Val134	0.51	Ile294	0.84
Leu135	2.17	Tyr312	1.20
Asp138	1.03	Tyr313	1.97
Tyr139	1.94	Ile316	0.75
Met142	1.42	Tyr320	0.92

As seen in Fig. 8a, the human κ-receptor binding pocket is comparatively narrow and deep. It is partially capped by the ECL2 β-hairpin. The binding antagonist reaches deep into the pocket to form ionic interactions with the Asp138 side chain. Asp138 is conserved in all opioid receptors, and mutagenesis studies suggest that it plays an essential role in anchoring positively charged κ-receptor ligands [17]. At the same time, protonated amines in the antagonist are also essential for opioid receptor antagonist activity, which suggests that the benzylic nitrogen atom should be retained in the structure modification. The sulfonyl group of the antagonist forms two hydrogen-bonds with Gln115 and Tyr313 (3.13 and 3.14 Å oxygen–oxygen for Gln115 and Tyr313, Fig. 8b). Gln115 was identified as a key residue in the binding mode of JDTic, and Tyr313 should be important in binding of RB-64 to the κ-receptor [1]. However, from Fig. 6 we found that the difference between the binding energy of these two residues is remarkable. The hydrogen-bond energy should be low because of long bond length. Gln115 contributes more through the hydrophobic interaction

with the biphenyl group. The R1 group is placed in a hydrophobic sub-pocket formed by the side chains of Tyr139, Met142, Trp287, Ile290, His291 and Ile316. Tyr139, His291 and Ile316 were identified as key residues in the binding of U50488 to the κ-receptor [2]. The biphenyl group interacts with the side chains of Leu135, Tyr312, Ile316, Tyr320 through hydrophobic interaction. Thr111, Gln115, Trp124 and Val134 form another sub-pocket, with R2 groups located in this pocket. The other five antagonists bind to κ-receptor in a mode similar to that of 22, and no more key residues were identified. However, the contribution of special residues to each complex differed depending on ligand structure.

A total of 16 key resides were identified from the energy decomposition method . We aligned the final conformations of these residues to the starting structure to investigate the deviation of active site residues, which may help us predict the binding mode of novel ligands, especially for agonists. The RMSD values are listed in Table 2. The RMSD of ligand counterpart was 0.56 (Fig. S2 in supporting information). The data from Table 1 show that Gln115, Leu135, Tyr139, Trp287 and Tyr313 deviate much more from the reference structure. Trp287 is conserved in GPCRs, and is thought to be a key part of the activation mechanism in many class A GPCRs [18]. These observations are pertinent to structure-based drug design.

Conclusions

In this work, docking, lipid bilayer simulations and calculations of binding free energies using the MM-GBSA method were performed to study the binding of six small molecule antagonists to the κ-receptor, and the results show that van der Waals energies play a key role in binding. Detailed analysis suggest that the ammonium group of the antagonist forms ionic interactions with the Asp138 side chain, which plays an essential role in anchoring the positively charged ligand. The biphenyl group reaches deep into the hydrophobic pocket and forms van der Waals interactions with Gln115, Ile316, etc. Investigation of the deviation of the active site residues showed that Gln115, Leu135, Tyr139, Trp287 and Tyr313 deviate greatly from the reference structure.

Acknowledgments The authors gratefully acknowledge financial support from the Natural Science Foundation of China (No. 21071021) and the Fundamental Research Funds for the Central Universities.

References

1. Wu H et al (2012) Structure of the human kappa-opioid receptor in complex with JDTic. Nature 485(7398):327–332
2. Eguchi M (2004) Recent advances in selective opioid receptor agonists and antagonists. Med Res Rev 24(2):182–212
3. Patra MC et al (2012) Comparative modeling of human kappa opioid receptor and docking analysis with the peptide YFa. J Mol Graph Model 33:44–51
4. Law PY, Wong YH, Loh HH (2000) Molecular mechanisms and regulation of opioid receptor signaling. Annu Rev Pharmacol Toxicol 40:389–430
5. Metcalf MD, Coop A (2008) In: Rapaka RS, Sadée W (eds) Kappa opioid antagonists: past successes and future prospects drug addiction. Springer, New York, pp 395–431
6. Pfeiffer A et al (1986) Psychotomimesis mediated by kappa opiate receptors. Science 233(4765):774–776
7. Runyon SP et al (2010) Analogues of (3R)-7-hydroxy-N-[(1S)-1-{[(3R,4R)-4-(3-hydroxyphenyl) -3,4-dimethyl-1-piperidinyl]methyl}-2-methylpropyl)-1,2,3,4-tetrahydro-3-isoquinolinecarboxamide (JDTic). Synthesis and in vitro and in vivo opioid receptor antagonist activity. J Med Chem 53(14):5290–5301
8. Frisch MJ, Trucks GW, Schlegel HB, Scuseria GE et al (2009) Gaussian, Wallingford CT
9. Morris GM et al (2009) AutoDock4 and AutoDockTools4: Automated docking with selective receptor flexibility. J Comput Chem 30(16):2785–2791
10. Eswar N, Webb B, Marti-Renom MA, Madhusudhan MS, Eramian D, Shen MY, Pieper U, Sali A (2007) Comparative protein structure modeling using MODELLER. Curr Protoc Protein Sci Chapter 2:Unit 2 9. doi: 10.1002/0471140864.ps0209s50
11. Humphrey W, Dalke A, Schulten K (1996) VMD: visual molecular dynamics. J Mol Graph 14(1):33–38
12. Tom Darden DY, Pedersen L (1993) Particle mesh Ewald: An N·log(N) method for Ewald sums in large systems. J Chem Phys 98(12):10089–10092
13. Kollman PA, Massova I, Reyes C, Kuhn B, Huo S, Chong L, Lee M, Lee T, Duan Y, Wang W, Donini O, Cieplak P, Srinivasan J, Cheatham T, Case DA (2000) Calculating structures and free energies of complex molecules: combining molecular mechanics and continuum models. Acc Chem Res 33:889–897
14. Sanner MF, Olson AJ, Spehner J-C (1996) Reduced surface: an efficient way to compute molecular surfaces. Biopolymers 38(3):305–320
15. Onufriev A, Bashford D, Case DA (2000) Modification of the generalized born model suitable for macromolecules. J Phys Chem B 104(15):3712–3720
16. Verhoest PR et al (2011) Design and discovery of a selective small molecule kappa opioid antagonist (2-methyl-N-((2′-(pyrrolidin-1-ylsulfonyl)biphenyl-4-yl)methyl)propan-1-amine, PF-4455242). J Med Chem 54(16):5868–5877
17. Subramanian G et al (1998) Conformational analysis and automated receptor docking of selective arylacetamide-based κ-opioid agonists. J Med Chem 41(24):4777–4789
18. Standfuss J et al (2011) The structural basis of agonist-induced activation in constitutively active rhodopsin. Nature 471(7340):656–660